Limnol. Oceanogr., 47(2), 2002, 404–417

Assessment of the relationships between dominant cell size in natural phytoplankton communities and the spectral shape of the absorption coefficient

Áurea M. Ciotti,[1] *Marlon R. Lewis, and John J. Cullen*[2]
Centre for Environmental Observation Technology and Research (CEOTR), Department of Oceanography, Dalhousie University, Halifax, Nova Scotia, Canada B3H 4J1

Abstract

Size-fractionated chlorophyll concentration and phytoplankton absorption spectra were compared for a wide variety of natural communities. We found that, in general, when phytoplankton abundance increases, larger size-classes are added incrementally to a background of smaller cells. Natural phytoplankton communities from surface waters were explicitly characterized according to their dominant cell size and taxonomic group, and the relationships between this classification and the spectral shape of the phytoplankton absorption coefficient for the whole assemblage was described. By specifying the cell size of the dominant organism (pico-, ultra-, nano-, or microplankton), more than 80% of the variability in spectral shape of the phytoplankton absorption coefficient from 400 to 700 nm could be explained. This is a result of the strong covariation of the size of dominant organisms and several factors controlling the spectral shape of the phytoplankton absorption coefficient, such as pigment packaging and concentration of accessory pigments. Consequently, the shapes of phytoplankton absorption spectra can be reproduced using a spectral mixing model, where two spectra, representing the normalized phytoplankton absorption coefficients for the smallest and the largest cells found in our data set, are combined additively, using a single parameter to specify the complementary contribution of each. The differences between reproduced and measured spectra contain taxonomic and physiological information. This parameterization provides a simple tool for extracting ecological information from optical measurements. It can also be used in sensitivity analyses to describe the influence of the dominant cell size of phytoplankton on optical properties of surface waters.

Changes in phytoplankton species composition are a central feature of marine ecosystem dynamics. Description and prediction of these changes are important goals to many fields in oceanography. In recent years, great effort has been made to understand how changes in phytoplankton species composition can affect optical properties of surface waters (e.g., Morel 1997; Kahru and Mitchell 1998; Stuart et al. 1998; Stramski et al. 2001). A major application of these results is the use of in situ optical instruments or remote sensing to observe variability of phytoplankton continuously or synoptically. This is a complicated topic because phytoplankton communities include species differing in size, shape, external and internal structures, and pigment composition. All these characteristics influence their interaction with the light field to some degree, so many factors must be considered to completely describe the optical properties of different communities of phytoplankton. A central goal is thus to determine how much information is required to use ocean color for discriminating different types or communities of phytoplankton (e.g., Garver et al. 1994). It is hoped that some factors can be ignored and others will covary so that a reduced set of parameters can describe how variability in phytoplankton communities alters the optical properties of surface waters.

Phytoplankton are but one determinant of ocean color. The spectrum of radiance emerging from the ocean depends on the spectral shape of the backscattering coefficient and the absorption coefficients of all optically active components (i.e., water, particles, and dissolved components), as well as on the spectral characteristics and geometrical distribution of the light field (Morel and Prieur 1977). The bulk backscattering coefficient in the ocean has been attributed principally to components other than phytoplankton, such as submicron particles and bacteria (Stramski and Kiefer 1991) and bubbles (e.g., Zhang et al. 1998). Spectral absorption thus will be the main optical property that can be used to distinguish phytoplankton communities, with the exception of the strong backscattering associated with blooms of coccolithophores (Balch et al. 1996) and *Trichodesmium* (Subramaniam et al. 1999).

Data from different optical platforms (Sathyendranath et al. 1994; Subramaniam and Carpenter 1994; Morel 1997), as well as comparisons of absorption spectra from laboratory (Johnsen et al. 1994) and field (Kirkpatrick et al. 2000), suggest that differences in pigment composition can in some cases be used to distinguish different taxonomic groups. In contrast, Garver et al. (1994) showed that the variability found in a large set of particulate absorption spectra from different environments could be explained by only two spectral components: material containing pigments (phytoplank-

[1] Present address: Instituto Oceanográfico da Universidade de São Paulo, IO-USP, Praça do Oceanográfico, 191-Cidade Universitária, São Paulo, SP, Brazil, 05508-900.

[2] Corresponding author (john.cullen@dal.ca).

Acknowledgments

This manuscript was greatly improved by numerous comments on earlier versions from S. Sathyendranath, P. Hill, and W. Miller. Two reviewers also provided helpful suggestions. Statistical advice was provided by K. R. Thompson. Data were kindly provided by C. Roesler and T. Cucci. Field data were obtained in collaboration with Satlantic Inc. We are thankful to R. Davis, M. MacDonald, J. G. MacIntyre, G. Maillet, S. Johannessen, and J.-P. Parkhill for valuable help with the field operations.

This study was funded by ONR, NASA, CSA, NSERC Research Partnerships, Satlantic, and NOAA. A.M.C also was funded by CNPq (Brazil).

Table 1. Locations, dates, and measurements.

Location	Date	Cruise	Measurements
Bedford Basin	Aug 1992	BBS92	Chl *a*, floristics, particulate absorption
Bedford Basin	Aug 1993	BBS93	Chl *a*, cell size, floristics, particulate absorption
Bedford Basin	Jul–Dec 1996 (weekly)	BBTS96	Chl *a* (total and size classes), floristics, particulate absorption
Bedford Basin	20–22 Aug 1996	BBS96	Chl *a* (total and size classes), floristics, particulate absorption
Oregon coast	Sep 1994	ORE94	Chl *a* (total and size classes), floristics, particulate absorption (total and size classes)
Bering Sea	Apr 1996	BS96	Chl *a* (total and size classes), particulate absorption (total and size classes)
Bering Sea	Jun 1997	BS97	Chl *a*, particulate absorption

ton) and material that does not (detritus), inferring that differences in the shape of phytoplankton absorption spectra for different communities of phytoplankton are too small to detect.

The absorption properties of phytoplankton are influenced by intracellular shading (pigment packaging) as well as by pigment composition. Packaging of pigments (*see* Duysens 1956), which is strongly related to cell size, has been shown to influence important optical relationships such as that between phytoplankton absorption and chlorophyll concentration (Bricaud et al. 1995; Cleveland 1995; Carder et al. 1999) and those between ratios of upwelling radiance (Carder et al. 1991) and diffuse attenuation coefficients (Mitchell and Holm-Hansen 1991). Radiative transfer calculations, in which distinct components of a plankton community are modeled (Mobley and Stramski 1997; Stramski et al. 2001), have also predicted that different sizes of phytoplankton species can produce changes in the relationship between ocean color and the amount of chlorophyll because of differences in packaging (*see also* Ciotti et al. 1999; Sathyendranath et al. 2001).

When large sets of data from laboratory and field are integrated to describe the changes in optical properties of phytoplankton with increasing chlorophyll concentration, it is observed that, on average, the changes in optical properties are consistent with both an increase of phytoplankton cell size and a decrease in accessory pigmentation (cf. Yentsch and Phinney 1989; Bricaud et al. 1995). These consistent trends of pigment packaging and the concentration of accessory pigments as a function of trophic status can explain prominent features in robust empirical relationships between optical properties of surface waters and chlorophyll concentration (Ciotti et al. 1999). Once these general trends are established, a possible path toward discriminating natural communities of phytoplankton bio-optically is to quantify deviations from these general relationships in terms of ecologically relevant optically based parameters. The approach can be developed and tested by measuring absorption spectra for phytoplankton communities that can be discriminated on the basis of taxonomic composition and cell size, then describing the effects of these different communities on relationships between optical properties.

Here, we analyze near-surface bio-optical data from a wide variety of natural situations to determine the degree to which different communities of phytoplankton, explicitly discriminated in terms of cell size and dominant taxa, quantitatively affect the shape of phytoplankton absorption spectra. The goal is to develop a parameterization of phytoplankton absorption that provides a simple tool to extract ecological information from optical measurements.

Methods

Approach—Bio-optical characteristics of surface samples were measured in three different regions: waters off the coast of Oregon, shelf waters of the southeastern Bering Sea, and waters of Bedford Basin (Nova Scotia, Canada), the latter being sampled on several occasions (Table 1). Surface samples were collected with a clean bucket or a Niskin bottle closed just below the surface. The sampling design is fully described by Ciotti (1999). A simple classification, based on size and dominant taxa, was developed to provide a quantitative context for describing variability of phytoplankton communities in these waters. Phytoplankton were classified by size (modified from Sieburth et al. 1978) in two steps (*see details in Fig. 1*): (1) the ''dominant size fraction'' was determined using physical separation of chlorophyll into size fractions; (2) using microscopic or flow cytometric analysis of the dominant size fraction, ''dominant cell size'' was assigned to the dominant organism present in this fraction (i.e., the organism or group with the highest product of cell number and cell area in cross section). When chlorophyll size fractionation was not available, the dominant size fraction was established through microscopic analysis, sizing, or both and enumeration of particles using a Coulter Counter. When the dominant cells are in chains or colonies, the dominant cell size can be smaller than the dominant size fraction.

Pigments—Chlorophyll *a* (Chl *a*, mg m^{-3}), corrected for phaeopigments, was determined using a calibrated Turner Designs 10-005R fluorometer. Samples collected on GF/F filters were extracted at -10°C or below, for at least 24 h in precooled 90% acetone : DMSO solution (6 : 4 by volume, Shoaf and Lium 1976). Reported values are averages from triplicates.

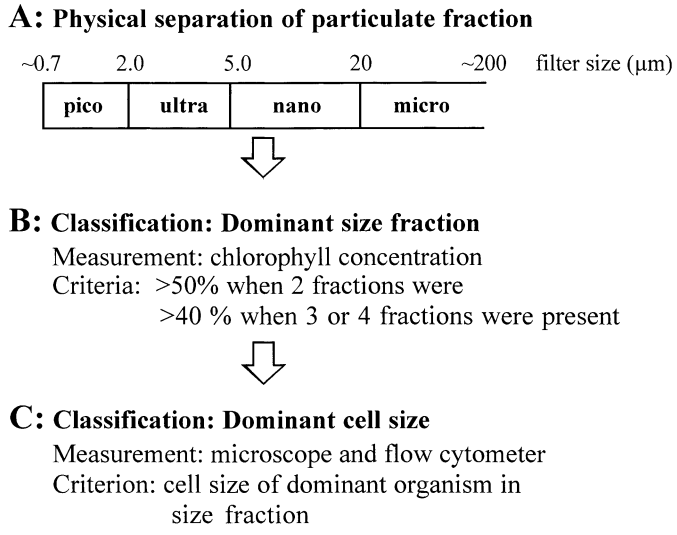

Fig. 1. Procedures followed to discriminate among different communities. (A) Samples were physically separated in four size ranges: picoplankton (<2 μm, collected on a GF/F filter; nominal pore size 0.7 μm), ultraplankton (between 2 and 5 μm), nanoplankton (between 5 and 20 μm), and microplankton (>20 μm). (B) Chlorophyll concentration was measured fluorometrically in each size range. The dominant size fraction was defined as the one containing more than 50% of the total chlorophyll when only two ranges were present, or the one containing more than 40% of the total chlorophyll when more than two ranges were present. Samples that did not meet either criterion were excluded from the analysis. (C) The dominant organism within the dominant size fraction was identified through either microscopic or flow cytometric analyses. That is, only the cells retained in the dominant size fraction were counted and sized. The dominant organism or group within the designated dominant size fraction was determined by using the product of cell number and cross-sectional area of the cells.

Particulate absorption—Samples were concentrated onto GF/F filters and analyzed immediately after filtration or preserved in liquid nitrogen for a maximum of 2 months until analysis. Absorption of particulate material was determined following the method described by Mitchell and Kiefer (1983). Two different Cary 3 dual-beam spectrophotometers were used. For all samples, except those from the Oregon cruise, a pathlength amplification correction (beta) was determined using monospecific cultures (Mitchell 1990). For the Oregon cruise samples (courtesy of C. Roesler), beta was determined as in Roesler (1998). Sample filters were scanned against a blank filter taken from the same lot. Blank and sample filters were then extracted with pure methanol (Kishino et al. 1985) and rinsed with 100 ml of 0.2 μm filtered artificial seawater. Each scan was smoothed using a 5-nm running average and corrected for differential scattering (setting the mean absorption between 740 and 750 nm to zero, *but see* Tassan et al. 2000), the volume filtered, and area of the filter. Phytoplankton absorption was computed as the difference between scans before (total particulate) and after (detritus) methanol and water extraction. Reported values are averages from duplicates or triplicates.

Size-fractionated Chl a *and particulate absorption*—Filtrates from 20-, 5-, and 2-μm Poretics® or Nuclepore® polycarbonate filters (47 mm diameter) were concentrated onto GF/F glass fiber filters (nominal pore size 0.7 μm). Filtration using polycarbonate filters was driven by gravity or very low pressure (less than ~25 mm Hg), and several filters were used for each fraction to avoid clogging (maximum volume 400–500 ml filter^{-1}). The concentration of Chl *a* and particulate absorption in each size fraction was determined as follows: total refers to whole sample; microplankton (cells >20 μm) refers to total minus the 20-μm filtrate; nanoplankton (cells between 5 and 20 μm) refers to the 20-μm filtrate minus the 5-μm filtrate; ultraplankton (cells between 2 and 5 μm) refers to the 5-μm filtrate minus the 2-μm filtrate; and picoplankton (cells <2 μm) refers to the 2-μm filtrate. Reported values are averages from triplicates.

Spectral shape of phytoplankton absorption—For comparison among the different communities, phytoplankton absorption spectra ($a_{ph}(\lambda)$, m^{-1}) were normalized using the mean absorption ($\langle a_{ph} \rangle$, m^{-1}) computed between 400 and 700 nm,

$$\langle a_{ph} \rangle = \frac{1}{301} \sum_{\lambda=400}^{700} a_{ph}(\lambda) \cdot \Delta\lambda \quad (1)$$

where $\Delta\lambda = 1$ nm. For comparison with previous work, the phytoplankton absorption spectra were also normalized to the sum of chlorophyll plus phaeopigment concentrations (mg m^{-3}) to yield pigment-specific phytoplankton absorption ($a^*_{ph}(\lambda)$, m^2 mg^{-1}).

Flow cytometric analyses—Samples from the Oregon cruise were analyzed with a FACScan flow cytometer (Becton Dickinson) equipped with a 15-mW air-cooled argon laser (488 nm). For all detected particles, forward light scatter, 90-degree light scatter, phycoerythrin fluorescence emission (560–590 nm), and chlorophyll fluorescence emission (>650 nm) were processed (data courtesy of T. Cucci, Bigelow Laboratory). The volume of the sample analyzed was estimated by the addition of a known concentration of fluorescent microspheres (10 μm diameter) to each sample immediately before analysis. Samples were run at ~10–12 μl min^{-1}. Different groups in each sample were identified by using a combination of forward light scattering and red and orange fluorescence (Yentsch et al. 1983).

Microscopic analyses—An inverted microscope was used to examine samples fixed with a solution (1% final concentration) of 25 g paraformaldehyde dissolved in 100 ml of hot (80°C) 25% glutaraldehyde, clarified with few drops of 1 N NaOH. The cells in the sample were concentrated using sedimentation chambers and scanned using ×100 and ×400 magnification. The lower limit of detection was about 3 μm. Only cells within the dominant Chl *a* size fraction (*see Fig. 1*) were counted and sized, and the dominant genera were chosen by computing the product of cell number and an average cross-sectional area for each group identified in that fraction. It is important to note that the reported cell sizes from the microscopic analyses tended to underestimate the actual sizes because of fixative effects and that the reduction in size depends on the organism and storage time. Here however, we cannot assess these changes. Thus, as a first ap-

Table 2. Summary of the distinct communities of phytoplankton characterized in the combined data sets. Name describes dominant cell size range (P is pico, U is ultra, N is nano, and M is micro) and species or groups of the dominant organism. na, not available. For details on cruises, refer to Table 1.

Name	Cruise	No. of samples	Dominant Chl *a* fraction	Chl *a* conc. range (mg m^{-3})	Main genera or group	Dominant cell size	Classification
P-Pro	ORE94	7	pico	<0.3	*Prochlorococcus*	pico	Flow cytometer
P-Syn	ORE94	9	pico	0.5–0.6	*Synechococcus*	pico	Flow cytometer
U-flag1	BBS92	20	na	2.5–7.5	Flagellates	ultra	Microscope
U-flag2	ORE94	4	ultra	1.5–1.7	Cryptomonads	ultra	Flow cytometer
U-flag3	BBS96	14	ultra	4–8	Flagellates	ultra	Microscope
U-unkw	BS96	9	ultra	0.5–0.7	Unknown	assumed ultra	Chl *a* fractionation
U-Phae	BS97	12	na	2–7	*Phaeocystis*	assumed ultra	HPLC and literature
N-din	BBS93	7	nano	6–36	*Prorocentrum*	nano	Coulter
N-cfd1	BS96	8	micro	0.9–2.3	*Chaetoceros*	nano	Microscope
N-cfd2	BBTS96	5	na	9–10	*Skeletonema*	nano	Microscope
N-cfd3	BBTS96	3	micro	17–30	*Skeletonema*	nano	Microscope
N-flag	BBTS96	11	nano	6.5–8	Flagellates	nano	Microscope
M-din1	BBS93	8	micro	27–135	*Gonyaulax*	micro	Coulter
M-cfd1	ORE94	15	micro	8–20	*Pseudo-nitzschia* and *Lauderia*	micro	Microscope
M-din2	BBTS96	2	micro	8–16	*Prorocentrum*	micro	Microscope
M-cfd2	BBTS96	2	micro	3–15	*Thalassiosira*	micro	Microscope

proximation, we will consider that fixative effects did not interfere with our classification, but the results deriving from samples having cell sizes close to the upper or lower limit of a given size fraction must be interpreted with caution.

Particle size—Samples from the summer of 1993 in Bedford Basin were analyzed with a Coulter Multisizer II Particle Analyzer equipped with a 75-μm aperture. Lower and upper limits of detection were 3 and 50 μm, respectively.

Results

We gathered 140 surface-layer samples of phytoplankton absorption, of which 136 could be classified following our criteria (*see Fig. 1*). A summary of the classification is presented in Table 2.

Chl a *size fractions*—We observed that the relative contributions of the four different size classes to the total Chl *a* varied among the different sampling regimes (*see Table 1* for nomenclature). During ORE94, when Chl *a* decreased from as high as 20.7 mg m^{-3} near the coast to < 0.3 mg m^{-3} offshore, picoplankton Chl *a* remained approximately constant and the variability in total Chl *a* was explained by changes in the larger size classes (Fig. 2A). Samples from shelf waters of the Bering Sea (Fig. 2B) showed that the picoplankton fraction tended to increase slightly with total Chl *a*, as did the ultraplankton and nanoplankton fractions. The range of surface Chl *a* was 0.8 to 5.5 mg m^{-3}. In Bedford Basin during 3 d in August 1996, the dominant fraction was the ultraplankton (Fig. 2C). Chlorophyll in the picoplankton fraction was about one order of magnitude higher than in Oregon and in the Bering Sea, showing at most a weak tendency to increase with total Chl *a*, which varied between 3.9 and 11.7 mg m^{-3}. During the time series from July to December 1996 (Fig. 2D), the trend was the same as during the Oregon cruise; that is, picoplankton Chl *a* remained approximately constant, and the variability in total Chl *a* (from 1.5 to 32 mg m^{-3}) was explained by increases in the larger fractions of the total Chl *a*.

When Chl *a* size fractionations were not available, the dominant size fraction was chosen with the help of a microscope (BBS92 and the initial samples from BBTS96) and a Coulter Counter (BBS93). In the specific case of BS97, a large number of colonies of what was believed to be the prymnesiophyte *Phaeocystis* were observed in fresh samples from surface waters. Pigment determined by high-performance liquid chromatography analysis collected concurrently (J. P. Parkhill pers. comm.) showed high ratios of 19-hexanoyloxyfucoxanthin to Chl *a* and also Chl c_3, consistent with the presence of prymnesiophytes (Jeffrey and Wright 1994). We therefore assumed that this community was dominated by a *Phaeocystis* species in the ultraplankton size class (e.g., *P. pouchetti* have cells between 4 and 8 μm in length, Tomas 1997).

Spectra of phytoplankton absorption—For each region sampled, mean-normalized absorption spectra (*see Eq. 1*) for whole samples from surface waters varied in shape according to the dominant size fraction for Chl *a* (Figs. 3A, 4) or dominant cell size from microscopy (Fig. 5). As expected for normalized spectra influenced by pigment packaging, spectra for samples dominated by microplankton were relatively flat, and smaller size classes (e.g., picoplankton in Fig. 3A) showed stronger spectral variation, such as the peak near 440 nm.

Differences among phytoplankton absorption spectra classified according to dominant Chl *a* size fraction were ini-

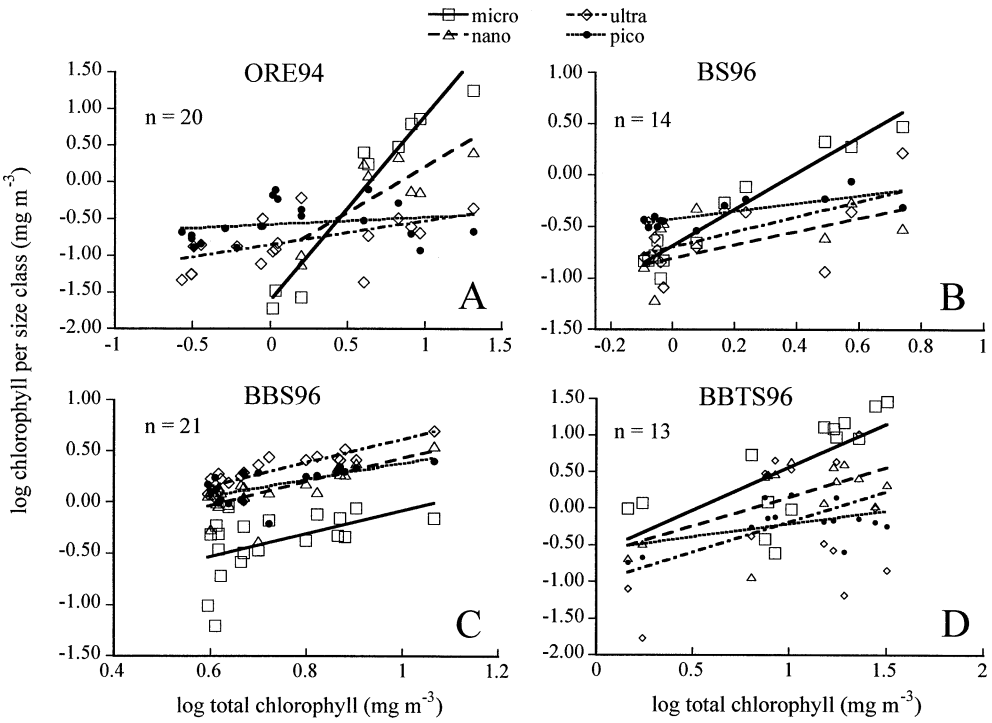

Fig. 2. Chlorophyll in size-fractions versus total chlorophyll for different data sets. (A) Oregon coast in 1994, (B) Bering Sea in April 1996, (C) 20–22 August 1996 in Bedford Basin, and (D) time series in 1996 in Bedford Basin, including the fall bloom. Samples are from the surface. Note that concentrations are in log scale. Lines are linear regressions on log-transformed data and only illustrate trends in the data.

tially tested with a nonparametric Kruskal–Wallis one-way analysis of variance. Measurements of normalized absorption at individual wavelengths were compared. Results for 440 nm are representative of those for most wavelengths between 400 and 700 nm. For ORE94 (Fig. 3A), normalized phytoplankton absorption at 440 nm from spectra grouped as picoplankton ($n = 16$), ultraplankton ($n = 4$), and microplankton ($n = 15$) were significantly different at the 0.05 level. During BS96 (Fig. 4A), however, the normalized phytoplankton absorption spectra classified as ultraplankton ($n = 9$) were not significantly different from spectra classified as microplankton based on size fractionation ($n = 8$); the latter were composed of chain-forming diatoms with small (nano) cells. During 1997 in the Bering Sea, only one group was sampled (Fig. 4B), so variability between spectra was not assessed.

Spectra from Bedford Basin were grouped by dominant cell size and averaged (Fig. 5). In general, the trends of normalized absorption with dominant cell size were consistent with those for dominant Chl *a* size fraction (i.e., larger sizes had flatter spectra). Statistical comparison of these spectra is incorporated in the analyses presented below.

Samples collected during ORE94 were also physically separated into the same size fractions as Chl *a* prior to analysis of particulate absorption (Fig. 3B). We observed the same trends comparing Fig. 3A and 3B; nonetheless, the variability within each size fraction was higher for the samples physically separated. This is probably a result of errors associated with the filter pad method because it is very sensitive to the amount of material concentrated on the filters (Mitchell 1990), and size-fractionated samples have less pigment than whole samples. In addition, spectra as in Fig. 3B, calculated by difference, are subject to propagation of error. Additional size fractionations were conducted on six samples from offshore, using filters with 1-μm pore diameter. The intention was to separate the influence of *Prochlorococcus* from that of *Synechococcus,* guided by the observations on fresh samples analyzed in real time by flow cytometry. Differences between these $<$1- and $<$2-μm fractions (Fig. 3C) could be attributed to relative contributions of these two groups and, thus, their respective sizes and pigment composition.

Influence of the different communities on the spectral shape of phytoplankton absorption—Combining all the sampling programs, 16 communities were characterized according to dominant Chl *a* size fraction, dominant cell size, and genus or taxonomic group of the dominant organisms (Table 2). The name given for each community specifies the dominant cell size and taxonomic group, and groups with the same names were numbered sequentially in order of sampling dates.

By grouping all the communities according to the cell size range of the dominant organism, we illustrate the relative influence of size on the shape of the absorption spectrum (compare Fig. 6A–D; means are presented in Fig. 6E). It is important to remember, however, that this classification refers to ranges of size, and there is still a degree of variability

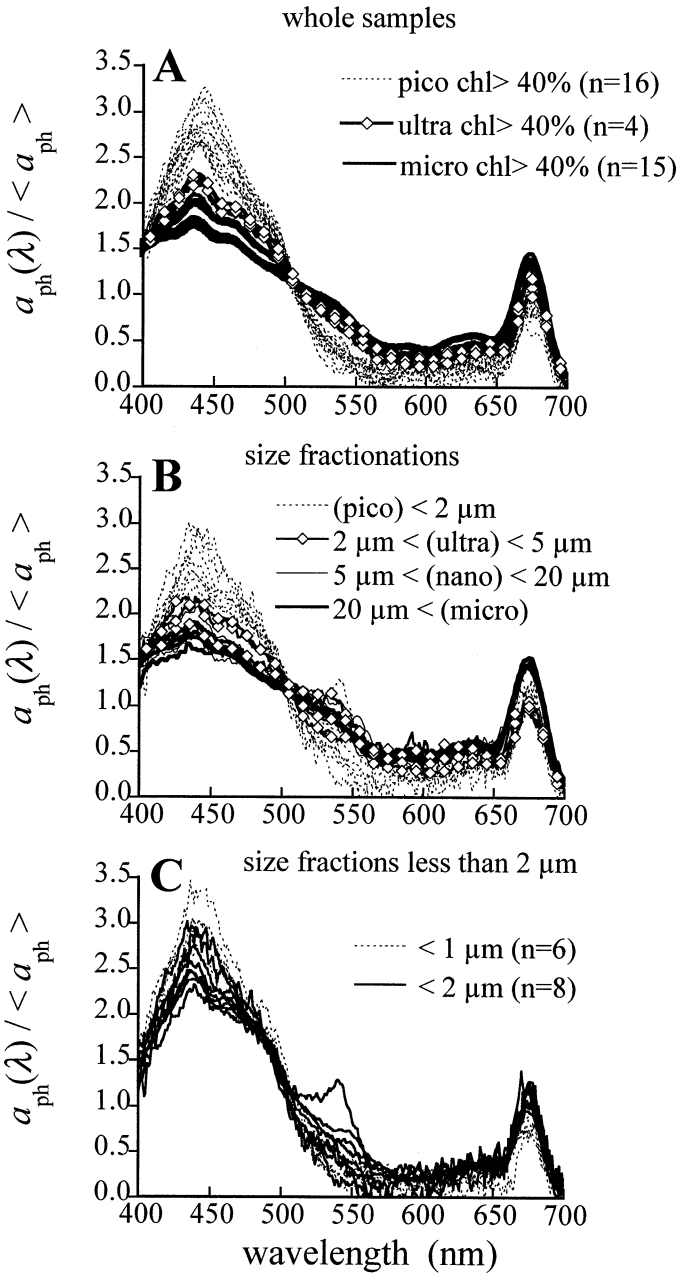

Fig. 3. (A) Phytoplankton absorption spectra measured during the Oregon cruise on whole surface samples. Spectra were normalized to the average phytoplankton absorption between 400 and 700 nm. Legend indicates the dominant Chl *a* size fractions (defined in Fig. 1). (B) Normalized phytoplankton absorption spectra measured directly for different size fractions collected on GF/F filters. (C) Comparison of absorption for size fractions from 14 stations using either 1- or 2-μm filters.

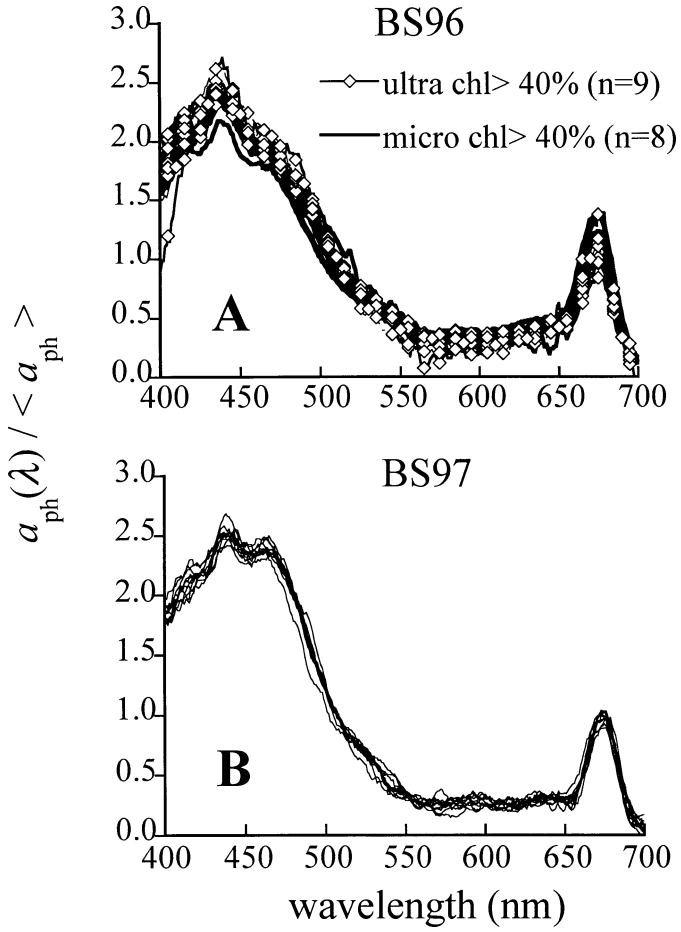

Fig. 4. Phytoplankton absorption spectra measured on whole surface samples collected in the southeastern Bering Sea. Spectra are normalized as in Fig. 3. (A) April 1996. Legend indicates the dominant chlorophyll size range. (B) Community dominated by *Phaeocystis* (*see text*), June 1997.

within each range associated with changes in size. For example, the nano-chain–forming diatoms found in Bedford Basin in the summer (N-cfd2) and in the Bering Sea (N-cfd1) were close to the lower limit attributed to this size range (i.e., 5 μm), whereas the nano-dinoflagellates found in 1993 during the red tide in Bedford Basin (N-din) were close to the upper limit of this range (i.e., 20 μm). The distinctions between the spectra classified as ultra- (Fig. 6B) and those classified as nanoplankton (Fig. 6C) were not strong, except in the samples collected in the Bering Sea in 1997 (where *Phaeocystis* was present), which had a distinct peak centered around 465 nm (Fig. 6B).

Within each size range, there was variability due to differences in pigment composition related to taxonomy. Samples dominated by ultraflagellates during the Oregon cruise (U-flag2, Fig. 6B) showed a shoulder centered around 545 nm that was associated with high numbers of *Synechococcus* (flow cytometer measured 1.59×10^5 cells ml^{-1}) and that probably resulted from a high concentration of phycoerythrin (*see* Moore et al. 1995; Morel 1997). In the nanoplankton fraction (Fig. 6C), peaks centered around 412 nm were present when *Skeletonema* spp. dominated. This was more noticeable during the summer in Bedford Basin. In the microplankton fraction (Fig. 6D), differences between diatom-dominated and dinoflagellate-dominated spectra were very small in the visible wavelengths. It is acknowledged that pigment packaging and concentration (Chl *a* and accessory pigments) can also vary with the physiological state of the community, but overall, the results illustrated well-known

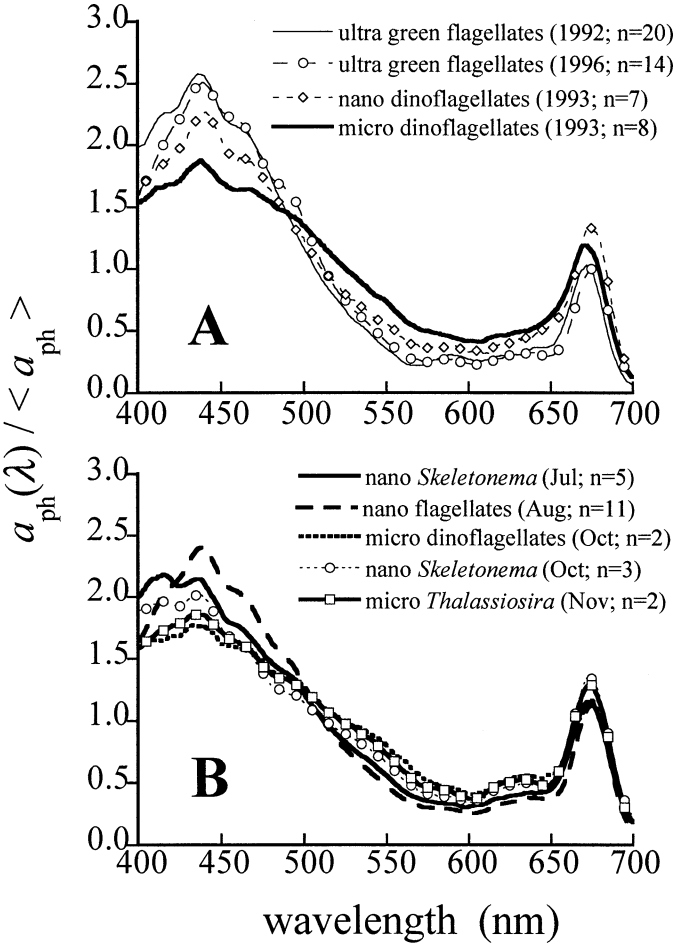

Fig. 5. Phytoplankton absorption spectra measured on whole surface samples collected at the surface in Bedford Basin. Spectra are normalized as in Fig. 3. Legends indicate the communities characterized according to cell size and dominant group (*see text*). Lines are averages for the number of samples (*n*) indicated in the legend. (A) August samples, 1992–1996. (B) 1996 time series.

trends (Fig. 6E): as the size of the dominant organism increases, the spectra flatten consistently with the increase in pigment packaging (Bricaud et al. 1995).

For comparison with previous work, absorption spectra of the 16 communities were also normalized to the concentration of Chl *a* plus phaeopigments ($a^*_{ph}(\lambda)$, Fig. 7). It is noteworthy that, although the trends observed in Fig. 6 were repeated, the variability within each cell size range was somewhat higher when reported as $a^*_{ph}(\lambda)$. This might be attributed to a number of causes, including real differences

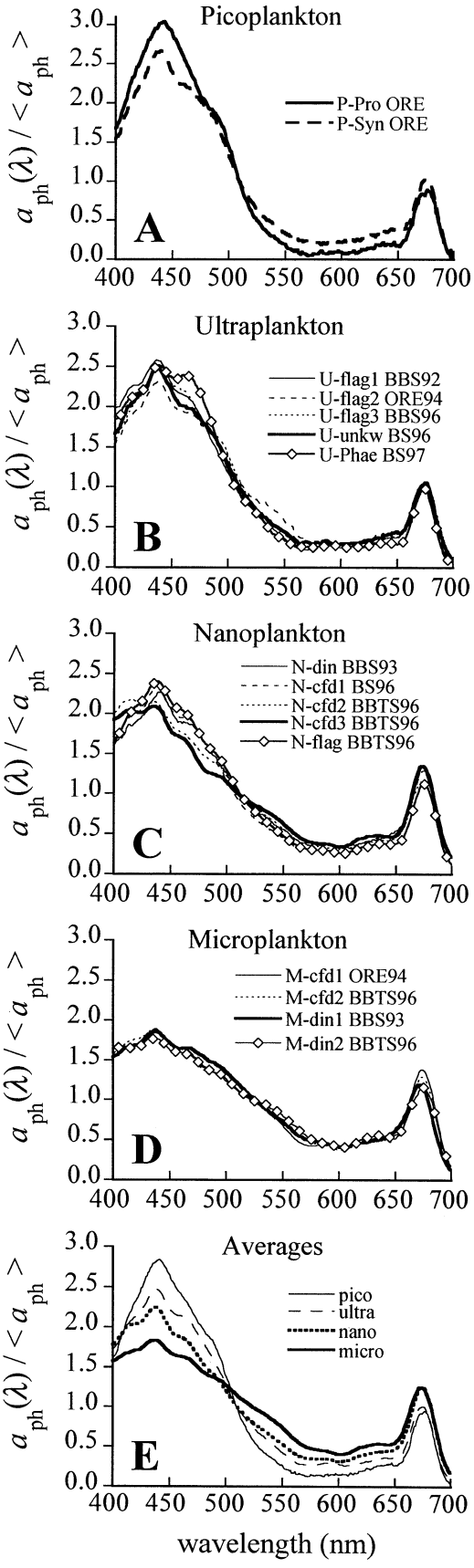

→

Fig. 6. Spectral shape of phytoplankton absorption coefficient for whole-water surface samples collected in all experiments, according to cell size range of the dominant organism (*see Fig. 1*). (A) Picoplankton. (B) Ultraplankton. (C) Nanoplankton. (D) Microplankton. (E) Average for each range. Legends indicate the communities characterized in Table 2, where information on sampling and classification is provided.

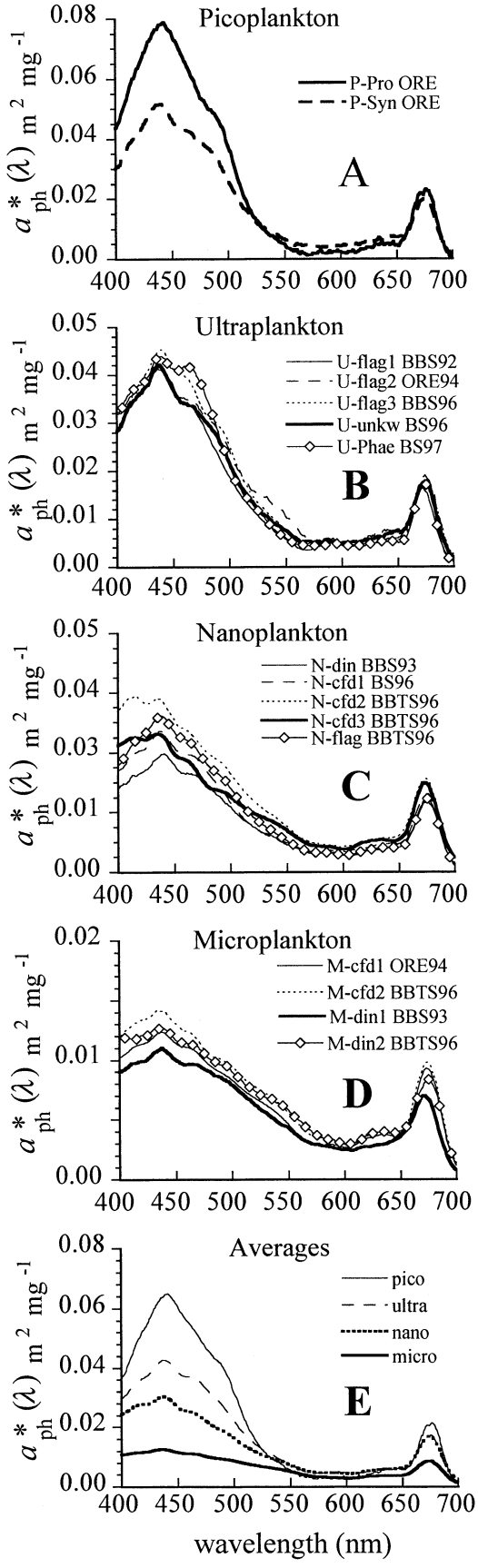

Fig. 7. Same as in Fig. 6 except that phytoplankton absorption spectra were normalized by Chl *a* plus phaeopigments. Note changes in the scale on *y*-axes.

in packaging and the concentration of accessory pigments. Biases in the measurement of Chl *a* plus phaeopigments due to accessory pigments can lead to either under- or overestimation of $a^*_{ph}(\lambda)$. Different degrees of activity of chlorophyllases (especially where diatoms dominate the community, Jeffrey and Hallegraeff 1987) can also produce biases associated with the longer time required for concentrating samples for particulate absorption samples, leading to more degradation of pigment for absorption vs. Chl *a* measurements (e.g., Stramski 1990). Correction for pathlength amplification seems not to be a factor, because the spectra from Oregon, which were calculated using a different method (Roesler 1998), are consistent with the others.

Quantification of the effects of cell size—Inspection of Figs. 6, 7 suggests that, despite the potential influence of the different accessory pigments on the phytoplankton absorption coefficient, a metric descriptor of the size of the dominant organism could effectively explain the variability in the shape of phytoplankton absorption spectra for surface assemblages. The dominant cell size range can be used as a proxy for many changes acting together, particularly pigment packaging and the concentration and composition of accessory pigments (Yentsch and Phinney 1989; Stuart et al. 1998; Ciotti et al. 1999). Therefore, when we refer to the effects of cell size, we are actually referring to the combined effects of a group of variables.

To evaluate the degree to which the cell size range of the dominant phytoplankton can explain the shape of the absorption spectrum, we conducted regression analyses using qualitative, categorical variables (Mendenhall and Sincich 1993) to identify the four size ranges. Like analysis of variance, regression with qualitative variables compares variability within and between groups, estimating how much of the variability in the dependent variable (in this case, normalized phytoplankton absorption) can be explained by the independent variable (dominant cell size). For each of 301 wavelengths between 400 and 700 nm, the following linear model was used.

$$a_{\langle ph\rangle}(\lambda) = \beta_0(\lambda) + \beta_1(\lambda)x_1 + \beta_2(\lambda)x_2 + \beta_3(\lambda)x_3 \quad (2)$$

The dependent variable, $a_{\langle ph\rangle}(\lambda)$ (i.e., $a_{ph}(\lambda)/\langle a_{ph}\rangle$, *see Eq. 1*), is normalized phytoplankton absorption at wavelength λ for each one of the 16 communities (Fig. 6). The qualitative (also called ''dummy'') variables for each normalized spectrum are x_1, x_2, and x_3, which were set according to the corresponding dominant cell size as follows.

For picoplankton,	$x_1 = 0$,	$x_2 = 0$, and	$x_3 = 0$.
For ultraplankton,	$x_1 = 1$,	$x_2 = 0$, and	$x_3 = 0$.
For nanoplankton,	$x_1 = 0$,	$x_2 = 1$, and	$x_3 = 0$.
For microplankton,	$x_1 = 0$,	$x_2 = 0$, and	$x_3 = 1$.

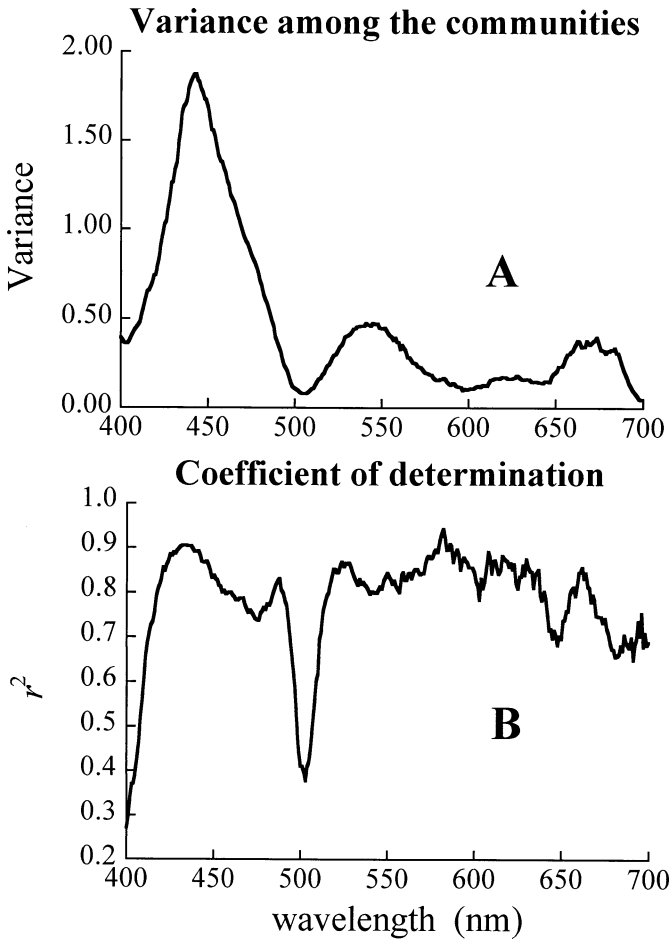

Fig. 8. Results of the regression analyses for 301 wavelengths (Eq. 2). (A) Initial variance of the data set (16 different communities). (B) Variability of the data explained by predefining cell size range of the dominant organism.

The parameters $\beta_0(\lambda)$ to $\beta_3(\lambda)$ are estimated by the linear regressions. $\beta_0(\lambda)$ will be the estimated absorption for picoplankton (i.e., $a_{\langle ph\rangle}(\lambda) = \beta_0(\lambda)$ when x_1, x_2, and $x_3 = 0$), $\beta_0(\lambda) + \beta_1(\lambda)$ is the estimated absorption for ultraplankton, $\beta_0(\lambda) + \beta_2(\lambda)$ is the estimated absorption for nanoplankton, and $\beta_0(\lambda) + \beta_3(\lambda)$ is the estimated absorption for microplankton. Note that $\beta_0(\lambda)$ represents the intercept of the regression, so the model assumes that the spectral shape for each other fraction can be described as a linear combination of the picoplankton spectrum and another shape. By running the analysis for the wavelengths between 400 and 700 nm, we generated the expected spectral shapes for the four size classes. These are equivalent to the average spectra for each group (Fig. 6E).

The initial variance among the 16 normalized spectra is shown in Fig. 8A, along with the coefficient of determination (r^2) at each wavelength (Fig. 8B), representing the variance in the absorption coefficient explained by the model at each wavelength. Note that the model explained more than 80% of the variability in most wavelengths. In other words, by knowing the cell size range of the dominant organism in the community, one can predict the shape of phytoplankton absorption spectra, accounting for more than 80% of the variance. Thus, these results strongly suggest that the dominant cell size in the community can be used to explain the variability of the absorption coefficient for distinct phytoplankton communities. Note that values for r^2 are relatively low for wavelengths around 500 nm because the original normalized spectra varied little in that range (*see Fig. 6E*).

Estimation of a ''size'' parameter from the phytoplankton absorption coefficient—The regular variation of spectral shapes from picoplankton to microplankton (Fig. 6E) and the results of the previous section (Fig. 8) suggest that the normalized absorption spectrum for each of 16 phytoplankton communities could be reconstructed with a linear combination of two spectra representing complementary contributions of the smallest and largest cell sizes found in our data set, so that

$$\hat{a}_{\langle ph\rangle}(\lambda) = [S_{\langle f\rangle} \cdot \bar{a}_{\langle pico\rangle}(\lambda)] + [(1 - S_{\langle f\rangle}) \cdot \bar{a}_{\langle micro\rangle}(\lambda)] \quad (3)$$

$\bar{a}_{\langle pico\rangle}(\lambda)$ and $\bar{a}_{\langle micro\rangle}(\lambda)$ are the ''basis vectors'' or shapes corresponding to the normalized absorption spectra for the smallest and largest cells (*see Table 3*), and the size parameter $S_{\langle f\rangle}$ is a magnitude constrained to vary between zero and 1.0 because we are considering the basis vectors to be the two possible extremes in size. Note that $\bar{a}_{\langle pico\rangle}(\lambda)$ is a spectrum for the average of all samples dominated by *Prochlorococcus*; thus, it differs from the spectral shape for picoplankton described in the previous analysis, which used the average spectrum for all samples dominated by picoplankton, including *Prochlorococcus* and *Synechococcus.* For $\bar{a}_{\langle micro\rangle}(\lambda)$ we used the average of all the samples dominated by microplankton-sized organisms.

The size parameter is estimated as the value of $S_{\langle f\rangle}$, which minimizes the sum of squared differences between a measured normalized spectrum, $a_{\langle ph\rangle}(\lambda)$, and the estimate, $\hat{a}_{\langle ph\rangle}(\lambda)$, for the 301 wavelengths from 400 to 700 nm. A least-squares routine (linear regression subjected to constraints on the value of $S_{\langle f\rangle}$, *see* Graham 1981) is used to fit any observed normalized phytoplankton absorption spectrum to Eq. 3 by adjusting the value of $S_{\langle f\rangle}$ between zero and 1.0, yielding (1) an estimate of the size parameter for the spectrum and (2) a reconstructed spectrum consistent with the size parameter. Estimated values of $S_{\langle f\rangle}$ for our 16 communities are presented in Table 4, and reconstructed spectra are compared with original spectra in Fig. 9. The approach can be used on any normalized absorption spectrum: tests on a number of published spectra showed that each could be reproduced well as a linear combination of the two basis vectors in Table 3, specified by size parameter $S_{\langle f\rangle}$ (data not shown).

Discussion

It is already well established that trends in the composition of phytoplankton communities can be related to local trophic status (Margalef 1978; Kiørboe 1993). In oligotrophic environments, phytoplankton biomass is dominated by prokaryotic cells (Chisholm 1992), which are small and have characteristic pigmentation (Goericke and Repeta 1992;

Table 3. Basis vectors representing the normalized absorption for the smallest ($\bar{a}_{\langle pico \rangle}(\lambda)$, *Prochlorococcus*) and biggest ($\bar{a}_{\langle micro \rangle}(\lambda)$, average microplankton) cell sizes in our data set. Wavelength (λ) in nm. Basis vectors for $a^*_{ph}(\lambda)$ can be constructed by setting $\bar{a}_{\langle pico \rangle}(676)$ to 0.023 $m^2\ mg^{-1}$, $\bar{a}_{\langle micro \rangle}(674)$ to 0.0086 $m^2\ mg^{-1}$, and scaling for the other wavelengths accordingly.

λ	Pico	Micro	λ	Pico	Micro	λ	Pico	Micro	λ	Pico	Micro	λ	Pico	Micro
400	1.682	1.574												
402	1.734	1.584	462	2.526	1.623	522	0.544	1.013	582	0.111	0.459	642	0.191	0.528
404	1.800	1.600	464	2.455	1.616	524	0.522	0.992	584	0.072	0.452	644	0.174	0.526
406	1.890	1.617	466	2.402	1.606	526	0.486	0.977	586	0.073	0.452	646	0.197	0.528
408	1.978	1.633	468	2.331	1.592	528	0.448	0.959	588	0.073	0.449	648	0.176	0.538
410	2.057	1.654	470	2.281	1.568	530	0.391	0.944	590	0.099	0.443	650	0.168	0.549
412	2.162	1.669	472	2.205	1.542	532	0.375	0.927	592	0.070	0.433	652	0.160	0.574
414	2.269	1.674	474	2.136	1.509	534	0.336	0.909	594	0.095	0.424	654	0.217	0.605
416	2.327	1.684	476	2.063	1.481	536	0.305	0.888	596	0.085	0.416	656	0.244	0.655
418	2.398	1.697	478	2.049	1.459	538	0.292	0.868	598	0.090	0.406	658	0.286	0.720
420	2.457	1.708	480	1.998	1.437	540	0.288	0.847	600	0.086	0.401	660	0.381	0.798
422	2.533	1.710	482	1.930	1.415	542	0.261	0.826	602	0.068	0.400	662	0.437	0.889
424	2.614	1.716	484	1.918	1.399	544	0.245	0.806	604	0.078	0.403	664	0.520	0.979
426	2.663	1.737	486	1.897	1.387	546	0.214	0.785	606	0.069	0.408	666	0.660	1.068
428	2.749	1.763	488	1.867	1.377	548	0.194	0.764	608	0.090	0.416	668	0.716	1.147
430	2.804	1.793	490	1.812	1.367	550	0.187	0.737	610	0.096	0.429	670	0.824	1.207
432	2.840	1.812	492	1.776	1.349	552	0.138	0.711	612	0.094	0.443	672	0.846	1.243
434	2.915	1.827	494	1.701	1.338	554	0.137	0.682	614	0.084	0.458	674	0.816	1.249
436	2.947	1.830	496	1.648	1.319	556	0.111	0.653	616	0.105	0.473	676	0.891	1.227
438	2.978	1.834	498	1.522	1.301	558	0.094	0.626	618	0.128	0.487	678	0.869	1.174
440	3.014	1.824	500	1.439	1.271	560	0.095	0.604	620	0.119	0.495	680	0.812	1.096
442	3.032	1.800	502	1.373	1.242	562	0.070	0.580	622	0.126	0.499	682	0.741	1.004
444	3.011	1.771	504	1.270	1.222	564	0.053	0.555	624	0.138	0.504	684	0.605	0.893
446	2.965	1.741	506	1.162	1.196	566	0.076	0.535	626	0.146	0.514	686	0.496	0.767
448	2.937	1.712	508	1.040	1.169	568	0.064	0.514	628	0.135	0.521	688	0.372	0.635
450	2.888	1.685	510	0.961	1.141	570	0.043	0.501	630	0.175	0.525	690	0.278	0.516
452	2.816	1.667	512	0.886	1.118	572	0.050	0.487	632	0.189	0.532	692	0.215	0.409
454	2.783	1.650	514	0.794	1.096	574	0.051	0.478	634	0.176	0.535	694	0.113	0.323
456	2.706	1.641	516	0.734	1.075	576	0.065	0.475	636	0.203	0.534	696	0.075	0.253
458	2.655	1.631	518	0.665	1.057	578	0.067	0.468	638	0.190	0.535	698	0.047	0.200
460	2.590	1.631	520	0.617	1.035	580	0.084	0.464	640	0.190	0.532	700	0.009	0.158

Moore et al. 1995). Only under higher nutrient conditions (i.e., eutrophic environments) can larger cells compete for nutrients, grow, and complement the small size groups (Malone 1980; Yentsch and Phinney 1989; Chisholm 1992). These larger cells will belong to distinct groups of species depending on both environmental conditions and on the ability of these species to exploit light and nutrients effectively (cf. Margalef 1978). Our goal here was to illustrate and justify, with a diverse variety of field examples, that despite the physiological and taxonomic variability associated with changes in community structure of phytoplankton, variation in the spectral shape of their bulk absorption coefficient can be described by simple relationships, representing covarying changes in a suite of factors that influence the optical properties of phytoplankton. This covariation is well described by changes in dominant cell size.

The concept of increasing phytoplankton biomass by the addition of groups of larger species to a background of smaller species, proposed by Yentsch and Phinney (1989), appears to hold for natural communities from coastal waters off Oregon (Fig. 2A) and over the seasonal cycle in Bedford Basin (Fig. 2D). Some increase in the background of small cells with Chl *a* was observed in the Bering Sea 1996 cruise (Fig. 2B), but in this case, the data represented mainly two fixed stations (Ciotti 1999). Variability during the 3-d study in Bedford Basin (Fig. 2C) was an exception to the model of a constant background state, showing a substantial increase in the standing stock (Chl *a*) of the picoplankton fraction concomitant with total Chl *a*. This could be related to different controls on phytoplankton community structure in this anthropogenically altered environment where enrichment with nutrients is not necessarily associated with enhanced turbulence (cf. Margalef 1978; Kiørboe 1993). However, it is important to remember that these data represent changes in the Basin during 3 d only. When the longer time-series for size-fractionated Chl *a* is analyzed (Fig. 2D), the expected trend is observed, with the fall-bloom phytoplankton community dominated by larger cells.

It appears that the Yentsch and Phinney (1989) approach is appropriate for comparing effects of different communities of phytoplankton on the variability of optical properties in many parts of the ocean. However, the generalization may not hold for reduced time and spatial scales, for which changes are associated with patchiness or advection. In other words, generalizations concerning increases in phytoplankton cell size with Chl *a* depend on the scales of variability considered.

Despite differences in taxonomic composition and relative proportions of Chl *a* size fractions observed during the different sampling programs, the shape of the absorption spec-

Table 4. Results from a linear decomposition of the phytoplankton absorption spectra for the different communities (*see Table 2*) using a linear regression subjected to constraints (Eq. 3). The size factor $S_{\langle f \rangle}$ is estimated and varies from 1.0 to zero for small and large cell sizes, respectively; r^2 is the coefficient of determination between observed and estimated spectra for 301 wavelengths from 400 to 700 nm. nr, not relevant. The linear regression uses two basis vectors representing the minimum and maximum cell size found in our data set (Table 3). For reference, $\langle a^*_{ph} \rangle$, the average $a^*_{ph}(\lambda)$ for each community (400–700 nm) is presented. Spectra of $a^*_{ph}(\lambda)$ can be reconstructed for each community by substituting $S_{\langle f \rangle}$ into Eq. 3 and multiplying the result by $\langle a^*_{ph} \rangle$.

Community	$S_{\langle f \rangle}$	r^2	No. of samples	$\langle a^*_{ph} \rangle$ (m^2 mg^{-1})
P-Pro	1.000	nr	7	0.0259
P-Syn	0.663	0.993	9	0.0195
U-flag1	0.598	0.979	20	0.0160
U-flag2	0.369	0.992	4	0.0180
U-flag3	0.558	0.995	14	0.0181
U-unkw	0.491	0.992	9	0.0170
U-Phae	0.664	0.982	12	0.0175
N-din	0.287	0.987	7	0.0111
N-cfd1	0.370	0.981	8	0.0126
N-cfd2	0.266	0.963	5	0.0169
N-cfd3	0.151	0.954	3	0.0138
N-flag	0.442	0.995	11	0.0136
M-cfd1	0.002	0.989	8	0.0067
M-cfd2	0.014	0.993	15	0.0076
M-din1	0.025	0.987	2	0.0059
M-din2	0.000	0.990	2	0.0072

trum for whole phytoplankton assemblages seems to vary systematically with the cell size range of the dominant organism (Figs. 6, 7). The comparison of the 16 communities characterized in this study indicated that, when size range was specified (i.e., pico-, ultra-, nano-, and microplankton), >80% of the variability in the shape of absorption spectra between 400 and 700 nm could be explained (Fig. 8B). The systematic variability observed can be related to both pigment packaging and the composition of accessory pigments.

Pigment packaging (or self-shading) is a well-documented source of variability for phytoplankton absorption and is a positive function of both cell size and intracellular concentration of pigments (Bricaud and Morel 1986; Sathyendranath et al. 1987). For monospecific laboratory cultures grown in nutrient-replete media, cell diameter (d) correlates negatively with the concentration of intracellular pigments (c_i). This has been described as a strategy to minimize self-shading (*see* Agusti 1991), and a similar correlation is expected in the field. In natural environments, however, cell size can be positively correlated to the availability of nutrients (Yentsch and Phinney 1989), which in turn can be positively correlated with c_i (Geider et al. 1998). Pigment composition can also be related to nutrient availability (Claustre 1994) due to the competition among different taxa (i.e., prokaryotes are more important in oligotrophic environments, Chisholm 1992) and also to physiological responses, as the concentration of accessory pigments, including photoprotective, tend to be higher in low-nutrient waters (Allali et al. 1997; Stuart et al. 1998; *but see* Trees et al. 2000). In other words,

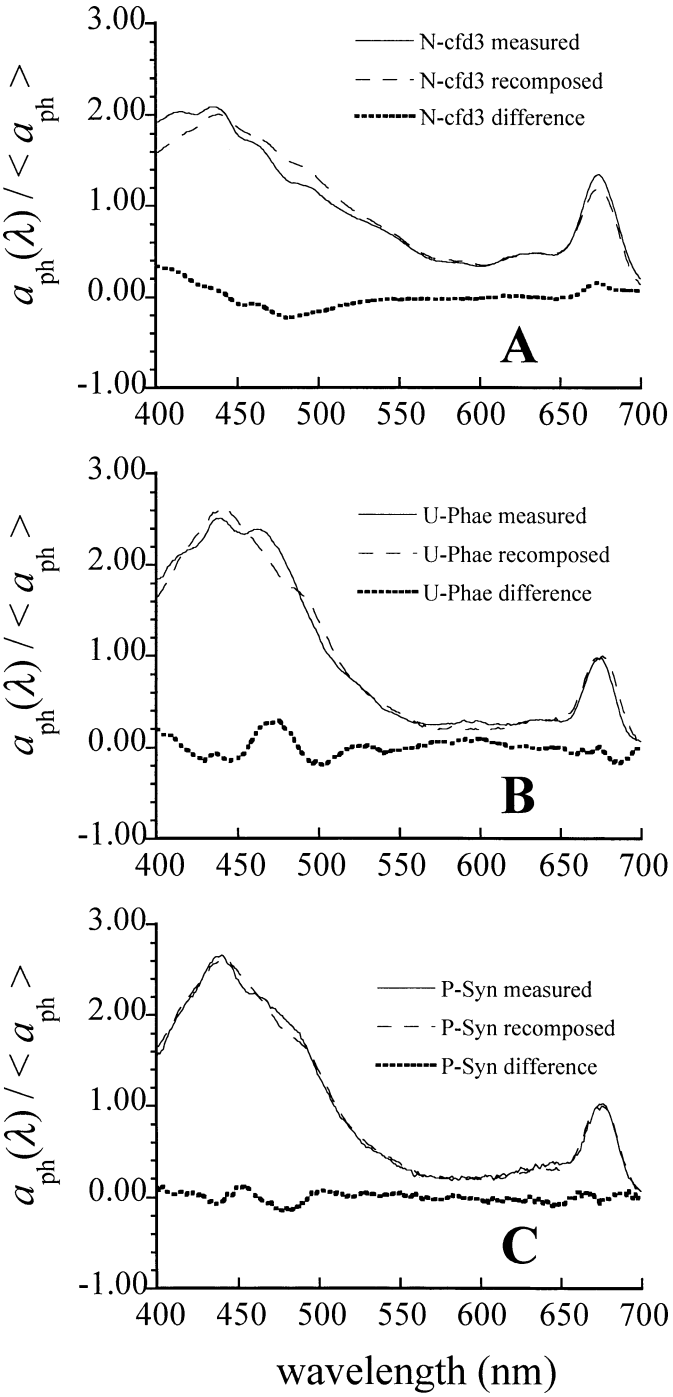

Fig. 9. Comparison of measured and recomposed (Eq. 3) spectra of normalized phytoplankton absorption. The recomposition uses a statistically determined size factor, $S_{\langle f \rangle}$, and two basis vectors, representing the average for the smallest and largest cell sizes found in our data set.

a suite of factors that controls the spectral shape of the absorption of phytoplankton shows a strong covariation with the size range of the dominant organism in the community. Because of that, a metric related to dominant cell size can be used as a parameter to explain a large portion of the variability observed in the spectral shape of the phytoplank-

ton absorption as influenced by hydrographic regime and nutrients.

Residual variability is expected to derive mainly from changes in pigment composition and intracellular concentration, which do not covary with cell size, and from variability in cell size within the predefined size ranges (*see Fig. 3C*). Consequently, the residuals contain some taxonomic and physiological information. Most of the residual variability was observed in narrow spectral bands (e.g., near 465 nm in Fig. 9B) that could be related to different accessory pigments (Bidigare et al. 1990; Hoepffner and Sathyendranath 1991). Very distinct peaks were observed in the ultraviolet region (not shown in the results) when both nano- and micro-dinoflagellates dominated the community, probably related to the presence of mycosporine-like amino acids (MAAs). Nevertheless, MAAs are not exclusive to dinoflagellates (e.g., Richardson et al. 1996), and peaks associated with MAAs in dinoflagellates can also be present or absent, depending on nutrient availability (Carreto et al. 1989).

Although simple parameterizations have already been proposed regarding changes in the absorption spectra of phytoplankton with Chl *a* (Bricaud et al. 1995; Lee et al. 1998; Sathyendranath et al. 2001), the parameterization proposed here has an explicit interpretation in ecological terms and no direct dependence on Chl *a*. The shapes of measured phytoplankton absorption spectra for the 16 different communities could be reproduced well ($r^2 > 0.95$; *see Fig. 9*) with a size factor, $S_{\langle f \rangle}$, describing the complementary contributions of two basis vectors (Table 4) representing the extrema in spectral shapes (from the smallest and largest dominant cell size observed). It is important to note that the shapes of the two extreme spectra are affected by the pathlength correction (or beta) factor applied in the calculation of particulate absorption. We have made the effort to concentrate the samples for particulate absorption to ensure a smaller range of beta per sample. Despite a number of recent works with conflicting results regarding the dependence of beta on species composition and wavelength (Moore et al. 1995; Roesler 1998; Tassan and Ferrari 1998), the overall conclusion of our results remain the same; that is, two extreme spectral shapes can be assigned to represent the smallest and largest cell sizes possible. The final spectra used in this approach can be easily changed as improvements in methodology reduce uncertainty in the measurement of $a_{ph}(\lambda)$.

Our description of phytoplankton absorption as a function of a size parameter describing the relative contributions of two spectral shapes could be implemented in inverse models for retrieving spectral absorption from ocean color. In inverse modeling techniques (e.g., Roesler and Perry 1995; Garver and Siegel 1997), ocean color spectra are fit to theoretical expressions that relate ocean color to inherent optical properties (IOPs), that is, absorption and backscattering. The values for the bulk IOPs, by definition, can be computed as the sum of the absorption or backscattering by all the optical components (i.e., water, particles, and dissolved material). These are represented by known values (e.g., absorption and backscattering by water) and by spectral shapes and magnitudes of the unknown components. The spectral shape for phytoplankton absorption is usually represented by a^*_{ph}; thus, the retrieved magnitude is chlorophyll plus phaeopigments. In the case of the parameterization of phytoplankton absorption suggested in this work, two basis vectors could be used and the retrieved magnitudes would be $S_{\langle f \rangle}$ and $\langle a_{ph} \rangle$ (i.e., the size parameter and the average value of phytoplankton absorption from 400 to 700 nm). Logically, the same approach can be done if one desires to use two extreme vectors for $a^*_{ph}(\lambda)$ and estimate pigment concentration instead (*see Table 3*).

Because the full natural range of variability in phytoplankton absorption can be effectively described with combinations $S_{\langle f \rangle}$ and $\langle a_{ph} \rangle$, covarying influences of phytoplankton communities on optical properties of surface waters can be studied by varying the size parameter and average absorption in sensitivity analyses. These studies would complement inverse models.

More work is needed to evaluate the feasibility of estimating $S_{\langle f \rangle}$ from remote sensing. Explicit consideration of spectral backscattering will be helpful. It also is important to establish how well the parameter $S_{\langle f \rangle}$ can be related to general features of phytoplankton communities or their ecology. Our results so far suggest a robust relationship between $S_{\langle f \rangle}$ and the cell size of the dominant organism. The retrieval of $S_{\langle f \rangle}$ from ocean color will thus have several applications in oceanography because many biogeochemical processes are directly related to the distribution of phytoplankton size classes in a given environment or time (Longhurst 1998).

References

AGUSTI, S. 1991. Allometric scaling of light absorption and scattering by phytoplankton cells. Can. J. Fish. Aquat. Sci. **48:** 763–768.

ALLALI, K., A. BRICAUD, AND H. CLAUSTRE. 1997. Spatial variations in the chlorophyll-specific absorption coefficients of phytoplankton and photosynthetically active pigments in the equatorial Pacific. J. Geophys. Res. **102:** 12,413–12,423.

BALCH, W. M., K. A. KILPATRICK, AND C. C. TREES. 1996. The 1991 coccolithophore bloom in the central North Atlantic. 1. Optical properties and factors affecting their distribution. Limnol. Oceanogr. **41:** 1669–1683.

BIDIGARE, R. R., M. E. ONDRUSEK, J. H. MORROW, AND D. A. KIEFER. 1990. In vivo absorption properties of algal pigments. Opt. Eng. **1302:** 290–302.

BRICAUD, A., AND A. MOREL. 1986. Light attenuation and scattering by phytoplankton cells: A theoretical modeling approach. Appl. Opt. **25:** 571–580.

———, M. BABIN, A. MOREL, AND H. CLAUSTRE. 1995. Variability in the chlorophyll-specific absorption coefficients of natural phytoplankton: Analysis and parameterization. J. Geophys. Res. **100:** 13,321–13,332.

CARDER, K. L., S. K. HAWES, K. A. BAKER, R. C. SMITH, R. G. STEWARD, AND B. G. MITCHELL. 1991. Reflectance model for quantifying chlorophyll *a* in the presence of productivity degradation products. J. Geophys. Res. **96:** 599–611.

———, F. R. CHEN, Z. P. LEE, S. K. HAWES, AND D. KAMYKOWSKI. 1999. Semianalytic moderate-resolution imaging spectrometer algorithms for chlorophyll *a* and absorption with bio-optical domains based on nitrate-depletion temperatures. J. Geophys. Res. **104:** 5403–5421.

CARRETO, J. I., S. G. DE MARCO, AND V. A. LUTZ. 1989. UV-absorbing pigments in the dinoflagellates *Alexandrium excavatum* and *Prorocentrum micans.* Effects of light intensity, p. 333–336. *In* T. Okaichi, D. M. Anderson, and T. Nemoto [eds.],

Red tides: Biology, environmental science, and toxicology. Elsevier.

CHISHOLM, S. W. 1992. Phytoplankton size, p. 213–238. *In* P. G. Falkowski and A. Woodhead [eds.], Primary productivity and biogeochemical cycles in the sea. Plenum Press.

CIOTTI, Á. M. 1999. Influence of phytoplankton communities on relationships between optical properties of coastal surface waters. Dalhousie University, Department of Oceanography.

———, J. J. CULLEN, AND M. R. LEWIS. 1999. A semi-analytical model of the influence of phytoplankton community structure on the relationship between light attenuation and ocean color. J. Geophys. Res. **104:** 1559–1578.

CLAUSTRE, H. 1994. The trophic status of various oceanic provinces as revealed by phytoplankton pigment signatures. Limnol. Oceanogr. **39:** 1206–1210.

CLEVELAND, J. S. 1995. Regional models for phytoplankton absorption as a function of chlorophyll *a* concentration. J. Geophys. Res. **100:** 13,333–13,344.

DUYSENS, L. N. M. 1956. The flattening of the absorption spectrum of suspensions as compared to that of solutions. Biochim. Biophys. Acta **19:** 1–12.

GARVER, S. A., AND D. A. SIEGEL. 1997. Inherent optical property inversion of ocean color spectra and its biogeochemical interpretation 1. Time Series from the Sargasso Sea. J. Geophys. Res. **102:** 18,607–18,625.

———, ———, AND B. G. MITCHELL. 1994. Variability in near-surface particulate absorption spectra: What can a satellite ocean color imager see? Limnol. Oceanogr. **39:** 1349–1367.

GEIDER, R. J., H. L. MACINTYRE, AND T. M. KANA. 1998. A dynamic regulatory model of phytoplankton acclimation to light, nutrients and temperature. Limnol. Oceanogr. **43:** 679–694.

GOERICKE, R., AND D. J. REPETA. 1992. The pigments of *Prochlorococcus marinus*: The presence of divinyl chlorophyll *a* and *b* in a marine procaryote. Limnol. Oceanogr. **37:** 425–433.

GRAHAM, A. 1981. Kronecker products and matrix calculus: With applications. Wiley.

HOEPFFNER, N., AND S. SATHYENDRANATH. 1991. Effect of pigment composition on absorption properties of phytoplankton. Mar. Ecol. Prog. Ser. **73:** 11–23.

JEFFREY, S. W., AND G. M. HALLEGRAEFF. 1987. Chlorophyllase distribution in ten classes of phytoplankton: A problem for chlorophyll analysis. Mar. Ecol. Prog. Ser. **35:** 293–304.

———, AND S. W. WRIGHT. 1994. Photosynthetic pigments in the haptophyta, p. 111–132. *In* J. C. Green and B. S. C. Leadbeater [eds.], The haptophyte algae. Claredon Press.

JOHNSEN, G., O. SAMSET, L. GRANSKOG, AND E. SAKSHAUG. 1994. In vivo absorption characteristics in 10 classes of bloom-forming phytoplankton: Taxonomic characteristics and responses to photoadaptation by means of discriminant and HPLC analysis. Mar. Ecol. Prog. Ser. **105:** 149–157.

KAHRU, M., AND B. G. MITCHELL. 1998. Spectral reflectance and absorption of a massive red tide off southern California. J. Geophys. Res. **103:** 21,601–21,609.

KIØRBOE, T. 1993. Turbulence, phytoplankton cell size, and the structure of pelagic food webs. Adv. Mar. Biol. **29:** 1–61.

KIRKPATRICK, G. J., D. F. MILLIE, M. A. MOLINE, AND O. SCHOFIELD. 2000. Optical discrimination of a phytoplankton species in natural mixed populations. Limnol. Oceanogr. **45:** 467–471.

KISHINO, M., M. TAKAHASHI, N. OKAMI, AND S. ICHIMURA. 1985. Estimation of the spectral absorption coefficients of phytoplankton in the sea. Bull. Mar. Sci. **37:** 634–642.

LEE, Z., K. L. CARDER, C. D. MOBLEY, R. G. STEWARD, AND J. S. PATCH. 1998. Hyperspectral remote sensing for shallow waters. I. A semianalytical model. Appl. Optics. **37:** 6329–6338.

LONGHURST, A. 1998. Ecological geography of the sea. Academic Press.

MALONE, T. C. 1980. Algal size, p. 433–463. *In* I. Morris [ed.], The physiological ecology of phytoplankton. Univ. of California Press.

MARGALEF, R. 1978. Life forms of phytoplankton as survival alternatives in an unstable environment. Oceanol. Acta **1:** 493–509.

MENDENHALL, W., AND T. SINCICH. 1993. A second course in business statistics: Regression analysis. Macmillan.

MITCHELL, B. G. 1990. Algorithms for determining the absorption coefficient of aquatic particulates using the quantitative filter technique (QFT). SPIE, Ocean Optics X **1302:** 137–148.

———, AND O. HOLM-HANSEN. 1991. Bio-optical properties of Antarctic Peninsula waters: Differentiation from temperate ocean models. Deep-Sea Res. **38:** 1009–1028.

———, AND D. A. KIEFER. 1983. Determination of absorption and fluorescence excitation spectra for phytoplankton. 5th Conf. Eur. Soc. Comp. Physiol. Biochem. **8:** 157–169.

MOBLEY, C. D., AND D. STRAMSKI. 1997. Effects of microbial particles on oceanic optics: Methodology for radiative transfer modeling and example simulations. Limnol. Oceanogr. **42:** 550–560.

MOORE, L. R., R. GOERICKE, AND S. W. CHISHOLM. 1995. Comparative physiology of *Synechococcus* and *Prochlorococcus*: Influence of light and temperature on growth, pigments, fluorescence and absorptive properties. Mar. Ecol. Prog. Ser. **116:** 259–275.

MOREL, A. 1997. Consequences of a *Synechococcus* bloom upon the optical properties of oceanic (case 1) waters. Limnol. Oceanogr. **42:** 1746–1754.

———, AND L. PRIEUR. 1977. Analysis of variations in ocean color. Limnol. Oceanogr. **22:** 709–722.

RICHARDSON, T. L., A. M. CIOTTI, J. J. CULLEN, AND T. VILLAREAL. 1996. Physiological and optical properties of *Rhizosolenia formosa* (Bacillariophyceae) in the context of open-ocean vertical migration. J. Phycol. **32:** 741–757.

ROESLER, C. S. 1998. Theoretical and experimental approaches to improve the accuracy of particulate absorption coefficients derived from the quantitative filter technique. Limnol. Oceanogr. **43:** 1649–1660.

———, AND M. J. PERRY. 1995. In situ phytoplankton absorption, fluorescence emission, and particulate backscattering spectra determined from reflectance. J. Geophys. Res. **100:** 13,279–13,294.

SATHYENDRANATH, S., L. LAZZARA, AND L. PRIEUR. 1987. Variations in the spectral values of specific absorption of phytoplankton. Limnol. Oceanogr. **32:** 403–415.

———, F. E. HOGE, T. PLATT, AND R. N. SWIFT. 1994. Detection of phytoplankton pigments from ocean color: Improved algorithms. Appl. Opt. **33:** 1081–1089.

———, G. COTA, V. STUART, H. MAASS, AND T. PLATT. 2001. Remote sensing of phytoplankton pigments: A comparison of empirical and theoretical approaches. Int. J. Remote Sens. **22:** 249–273.

SHOAF, W. T., AND B. W. LIUM. 1976. Improved extraction of chlorophyll *a* and *b* from algae using dimethyl sulfoxide. Limnol. Oceanogr. **21:** 926–928.

SIEBURTH, J. M., V. SMETACEK, AND J. LENTZ. 1978. Pelagic ecosystem structure: Heterotrophic compartments of the plankton and their relationship to plankton size fractions. Limnol. Oceanogr. **23:** 1256–1263.

STRAMSKI, D. 1990. Artifacts in measuring absorption spectra of phytoplankton collected on a filter. Limnol. Oceanogr. **35:** 1804–1809.

———, AND D. A. KIEFER. 1991. Light scattering by microorganisms in the open ocean. Prog. Oceanogr. **28:** 343–383.

———, A. BRICAUD, AND A. MOREL. 2001. Modeling the inherent

optical properties of the ocean based on the detailed composition of the planktonic community. Appl. Opt. **40:** 2929–2945.

STUART, V., S. SATHYENDRANATH, T. PLATT, H. MAASS, AND B. D. IRWIN. 1998. Pigments and species composition of natural phytoplankton populations: Effects on the absorption spectra. J. Plankton Res. **20:** 187–217.

SUBRAMANIAM, A., AND E. J. CARPENTER. 1994. An empirically derived protocol for the detection of blooms of the marine cyanobacterium *Trichodesmium* using CZCS imagery. Int. J. Remote Sens. **15:** 1559–1569.

———, ———, D. KARENTZ, AND P. G. FALKOWSKI. 1999. Bio-optical properties of the marine diazotrophic cyanobacteria *Trichodesmium* spp. I. Absorption and photosynthetic action spectra. Limnol. Oceanogr. **44:** 608–617.

TASSAN, S., AND G. M. FERRARI. 1998. Measurement of light absorption by aquatic particles retained on filters: Determination of the optical pathlength amplification by the ''transmittance–reflectance'' method. J. Plankton Res. **20:** 1699–1709.

———, ———, A. BRICAUD, AND M. BABIN. 2000. Variability of the amplification factor of light absorption by filter-retained aquatic particles in the coastal environment. J. Plankton Res. **22:** 659–668.

TOMAS, C. R. 1997. Identifying marine phytoplankton. Academic.

TREES, C. C., D. K. CLARK, R. R. BIDIGARE, M. E. ONDRUSEK, AND J. L. MUELLER. 2000. Accessory pigments versus chlorophyll *a* concentrations within the euphotic zone: An ubiquitous relationship. Limnol. Oceanogr. **45:** 1130–1143.

YENTSCH, C. M., AND OTHERS. 1983. Flow cytometry and cell sorting: A technique for analysis and sorting of aquatic particles. Limnol. Oceanogr. **28:** 1275–1280.

YENTSCH, C. S., AND D. A. PHINNEY. 1989. A bridge between ocean optics and microbial ecology. Limnol. Oceanogr. **34:** 1694–1705.

ZHANG, X., M. R. LEWIS, AND B. JOHNSON. 1998. The influence of bubbles on scattering of light in the ocean. Appl. Opt. **37:** 6525–6536.

Received: 30 November 2000
Accepted: 18 September 2001
Amended: 9 November 2001